The Relevance of the Location of Blocking Highs for Stratospheric Variability in a Changing Climate

BLANCA AYARZAGÜENA

Institut für Meteorologie, Freie Universität Berlin, Berlin, Germany

YVAN J. ORSOLINI

Norwegian Institute for Air Research, Kjeller, Norway

ULRIKE LANGEMATZ, JANNA ABALICHIN, AND ANNE KUBIN

Institut für Meteorologie, Freie Universität Berlin, Berlin, Germany

(Manuscript received 14 March 2014, in final form 1 October 2014)

ABSTRACT

Previous research shows that blocking highs (BHs) influence wintertime polar stratospheric variability through the modulation of the climatological planetary waves (PWs) depending on the BH location. BHs over the Euro-Atlantic sector tend to enhance the upward PW propagation, and those over the northwestern Pacific Ocean tend to reduce it. Future changes are examined in the response of the wave activity flux to the BH location and their relationship with wintertime stratospheric variability in transient simulations of ECHAM/Modular Earth Submodel System (MESSy) Atmospheric Chemistry (EMAC). After it is verified that EMAC can reproduce qualitatively well the geographical dependence of the BH influence on PW activity injection, it is shown that this dependence does not change in the future. However, an eastward shift of the pattern of the BH influence on PW propagation over the Pacific, a farther eastward extension of the pattern over the Atlantic Ocean, and an intensification of the wavenumber-1 component of the interaction between climatological and anomalous waves are detected. Changes in the upper-tropospheric jet and an intensification of the wavenumber-1 climatological wave due to a strengthening of the Aleutian low agree with these variations. The spatial distribution of future BHs preceding extreme polar vortex events is also affected by the slight modifications in the wave activity pattern. Hence, future BHs preceding strong vortex events tend to be more concentrated over the Pacific than in the past, where BHs interfere negatively with wavenumber-1 climatological waves. Future BHs prior to major stratospheric warmings are located in a broader area than in the past, predominantly over an extended Euro-Atlantic sector.

1. Introduction

Blocking highs (BHs) constitute one of the clearest examples of tropospheric precursors of wintertime polar stratospheric variability (e.g., Martius et al. 2009; Kolstad and Charlton-Perez 2011). They consist of anticyclonic quasi-stationary anomalies in the tropospheric pressure field that persist for several days to weeks, obstructing the westerly winds and midlatitude weather systems (Rex 1950). BHs also modify the upward propagation of tropospheric planetary waves and thereby influence the polar stratospheric circulation in winter (e.g., Polvani and Waugh 2004).

Early studies have already shown examples of major stratospheric warmings (MSWs) that were preceded by BHs (e.g., Julian and Labitzke 1965; Quiroz 1986). In the last decade, several authors have revisited this topic by analyzing the period covered by reanalysis data. Taguchi (2008) could not establish a statistical relationship between the occurrence of MSWs and the existence of preceding BHs. Following work focused on the impact of the geographical location of BHs on stratospheric variability, which helped to reconcile Taguchi's results with previous analyses (Martius et al. 2009; Castanheira and Barriopedro 2010; Woollings et al. 2010; Nishii et al.

Corresponding author address: Blanca Ayarzagüena, Institut für Meteorologie, Freie Universität Berlin, Carl-Heinrich-Becker-Weg 6-10, D-12165 Berlin, Germany.
E-mail: blanca.ayarzaguena@met.fu-berlin.de

DOI: 10.1175/JCLI-D-14-00210.1

2011, hereafter N11). Martius et al. (2009) showed that the distribution of BHs prior to MSWs determines the type of MSWs due to the BH influence on the upward propagation of planetary wave (PW) activity. Accordingly, MSWs characterized by a displacement of the vortex toward northern Europe are preceded by BHs over the Atlantic Ocean. MSWs resulting in a splitting of the vortex are preceded by Pacific BHs or simultaneous BHs over the Atlantic and Pacific Oceans Castanheira and Barriopedro (2010) confirmed the results of Martius et al. However, they also linked Pacific BHs to a destructive interference of climatological wavenumber-1 PW activity that sometimes is followed by an intensification of the polar vortex. This was also stated by Orsolini et al. (2009) and Nishii et al. (2010), but only for western Pacific BHs. This geographical dependence of the influence of BHs on the vertical PW propagation might explain the lack of statistical relationship between BHs and MSWs in Taguchi (2008). Similar conclusions to those of Castanheira and Barriopedro (2010) were derived by Woollings et al. (2010), but with contradictory results of the role of planetary wavenumbers 1 and 2 on the forcing of MSWs associated with European BHs. Later, N11 analyzed in detail the effects of BHs all over the extratropical Northern Hemisphere on the upward planetary wave propagation. They confirmed with more geographical detail the results about the effects of western Pacific and Euro-Atlantic BHs on wavenumber-1 and wavenumber-2 PW activity of Castanheira and Barriopedro (2010). They also stated that the BHs developing over Alaska and the eastern Pacific can either enhance or suppress the upward propagating wave activity depending on the case. Additionally, they quantified the importance of the interference between climatological and anomalous planetary waves in the total anomalous upward propagating wave activity related to BHs by applying a methodology based on the decomposition between a zonally varying time-mean state and local departures from this time-mean state (Nishii et al. 2009).

The influence of BHs on stratospheric variability has also been investigated in model simulations. In an early GCM study, Erlebach et al. (1996) related the development of an MSW to the previous occurrence of a BH over the eastern Atlantic. More recently, Bancalà et al. (2012) analyzed the distribution of BHs prior to the two types of MSWs in Middle Atmosphere ECHAM5 (MAECHAM5)/Max Planck Institute Ocean Model (MPI-OM) simulations. They found similar results to those from reanalysis data by Martius et al. (2009). Vial et al. (2013) examined in more detail the relation between MSWs and BHs in a simulation with L'Institut Pierre-Simon Laplace Coupled Model, version 5A (IPSL-CM5A), extending the analysis to other features related to BHs, such as changes in their duration associated with MSWs or possible effects of MSWs on blockings. In particular, they found that whereas BHs tend to last longer prior to the occurrence of MSWs (especially over the Eurasian sector), BHs forming after these events show a shorter duration. Additionally, Eurasian BHs shift westward after the occurrence of MSWs.

Because of the importance of BHs for atmospheric variability, some model studies have focused on possible changes of these phenomena in a future climate (Sillmann and Croci-Maspoli 2009; Woollings, 2010; de Vries et al. 2013; Dunn-Sigouin and Son 2013; Masato et al. 2013). All of them have found a general decrease in the frequency of BHs in the future over the two main areas, the Euro-Atlantic and Pacific sectors. Additionally, most of these studies found an eastward shift and a farther downstream extension of the areas with high frequency of BHs in the Euro-Atlantic sector in future winters (Sillmann and Croci-Maspoli 2009; de Vries et al. 2013; Masato et al. 2013). De Vries et al. (2013) related both changes in BHs to modifications of the mean climate, in particular, to a stronger and farther eastward extending tropospheric jet.

The purpose of this study is to go one step further and to investigate in which way future changes in BHs will influence stratospheric climate. Since the location of BHs in winter has been shown to have a strong impact on the upward propagation of planetary waves and thus, stratospheric variability, we focus on the analysis of possible future variations in the BH location and their effects on the above mentioned phenomena. To this end, the method of N11 was applied to output from transient simulations with the state-of-the-art chemistry climate model (CCM) ECHAM/Modular Earth Submodel System (MESSy) Atmospheric Chemistry (EMAC). First, we have validated the ability of EMAC to reproduce the observed geographical dependence of the BH influence on stratospheric variability in the recent past. In a second step, we have analyzed how this relationship changes in the future.

The structure of this paper is as follows: Section 2 describes the data and the methodology used in this work. The effects of the location of BHs on the upward propagation of PW activity and on the stratospheric variability in the past and the future of our model simulation are shown in section 3. In section 4, we discuss our results seeking for the possible causes that explain the future changes shown in section 3 and the robustness of the future signal. Finally, in section 5, we include a summary with the main conclusions derived from our work.

2. Data and methodology

a. Data description

The basis for the analysis of the abovementioned topic is provided by a transient simulation of the period 1960 to 2100 using EMAC. EMAC is a numerical chemistry and climate simulation system that includes submodels describing tropospheric and middle atmospheric processes (Jöckel et al. 2006). It uses the first version of the Modular Earth Submodel System (MESSy1, v1.10) to link multi-institutional computer codes. The core atmospheric model is the fifth-generation European Centre Hamburg general circulation model (GCM) (ECHAM5; Roeckner et al. 2006). Here we applied EMAC in a T42L39MA-resolution configuration, that is, with a spherical truncation of T42 (corresponding to a Gaussian grid of approximately 2.8° longitude × 2.8° latitude) and 39 hybrid levels up to 0.01 hPa (~80 km). Relevant submodels for the stratosphere are the chemistry module Module Efficiently Calculating the Chemistry of the Atmosphere version 1(MECCA1; Sander et al. 2005), the shortwave radiation scheme RAD4ALL–Freie Universität Berlin Radiation (FUBRAD) (RAD4ALL-FUBRAD; Nissen et al. 2007), and parameterizations for orographic and nonorographic gravity waves (Lott and Miller 1997; Hines 1997a,b).

A transient simulation was performed for the future representative concentration pathway 8.5 (RCP8.5) scenario that assumes an extreme future climate change, characterized by an additive anthropogenic radiative forcing of 8.5 $W m^{-2}$ exerted on Earth's climate system by the end of the twenty-first century (Meinshausen et al. 2011). The run includes forcings by ozone-depleting substances (adjusted A1 scenario; WMO 2007) and greenhouse gas concentrations (GHGs) following the specifications for this scenario. Sea surface temperatures (SSTs) and sea ice concentrations (SICs) were prescribed from a corresponding RCP8.5 simulation with the coupled atmosphere–ocean GCM ECHAM6/MPI-OM (Jungclaus et al. 2013). Other natural forcings such as solar variability are also included in the simulation. The quasi-biennial oscillation (QBO) is nudged to observations in the past and then repeated in the future. Future changes in BHs are deduced by the comparison between the last 40 winters of the run (denoted as future) with the first 40 winters (denoted as past). To obtain confidence in our conclusions the most relevant results are compared with a second EMAC transient run performed under a weaker climate change scenario (RCP4.5).

Daily data of this study have been filtered with an 8-day low-pass filter to retain only quasi-stationary circulation anomalies, since this study focuses on phenomena related to BHs (N11). The climatological daily mean of each period is computed as the mean of smoothed filtered data for each calendar day. The smoothing of data consists of a 31-day running average, so that a slow seasonal evolution of the circulation is obtained (Nishii et al. 2009). Daily anomalies of all fields are defined as the deviation of 8-day low-pass-filtered daily fields from the daily climatology.

b. Blocking highs

In this study BHs are identified following closely the method of Nakamura et al. (1997). BHs correspond to the 20 strongest centers of anticyclonic anomalies at the 250-hPa pressure level within 500 km of each grid point in the 40 extended winters [November–March (NDJFM)] of each period of study (1960/61–1999/2000 or 2060/61–2099/2100). To ensure the independence of two BHs, they have to be separated by more than 8 days.

Some remarks are added here about the appropriateness of this algorithm for our study. First, the number of BHs for each grid point is fixed in our computations (20 events; i.e., approximately one BH episode every two seasons). An analysis of the occurrence frequency of BHs is beyond the scope of this work. Moreover, when considering 20, 30, or 40 BHs, the main conclusions do not change. Additionally, while Nakamura et al. (1997) and N11 have already proven that events selected with this algorithm capture the characteristics of typical BHs and similar verifications have been done for our model data, it is not highly relevant if a few of the BHs identified in this study are not strictly BHs. We are mainly interested in the effects of strong circulation anomalies with an important influence on Rossby wave activity and thus on stratospheric variability. Finally, apart from the dynamical arguments indicated by N11 for the selection of the described algorithm, this method shows other advantages for the aim of this paper in comparison with the traditional methods by Dole and Gordon (1983) or Tibaldi and Molteni (1990). In particular, it allows us to obtain a two-dimensional distribution of BHs that is based on the climatology of each period and not on any arbitrary threshold for the strength of an event. We only specify a number of events selected at each grid point. Additionally, it is not restricted to any reference latitude or regions derived from the analysis of observations in the current climate. This is particularly convenient for a model study that compares past and future periods, since the behavior and distribution of BHs may change under different climate conditions because of changes, as well as model biases, in the background state (Scaife et al. 2010; Woollings 2010).

c. Upward wave activity propagation

The zonal-mean meridional eddy heat flux at 100 hPa at middle and high latitudes has been shown to be a good

measure of the tropospheric PW activity entering the stratosphere in winter (Hu and Tung 2003; Nishii et al. 2009). Anomalies of this metric averaged poleward of 45°N for the period from day −2 to day +7 around the peak of BHs are used here to characterize the fluctuations of the upward wave activity related to the occurrence of these events.

The characteristics of the total eddy heat flux anomalies have been analyzed based on a decomposition of the wave field into two different components: the climatological stationary waves (the wavy background flow) and the wave anomalies embedded in this flow. According to this decomposition the anomalous vertical wave activity flux can then be expressed as the sum of three terms (Nishii et al. 2009; Smith and Kushner 2012):

$$[v^*T^*]_a = [v^*_a T^*_a]_a + [v^*_c T^*_a] + [v^*_a T^*_c], \qquad (1)$$

where brackets and asterisks denote zonal mean and deviation thereof, respectively, v is the meridional wind, and T is the temperature. The subscripts a and c stand for anomalies and climatological values, respectively. Note that T^* and v^* are calculated for all wavenumber components using fast Fourier transform filters. The product of a certain wavenumber Fourier components of T^* and v^* gives the contribution to the heat flux of this wavenumber. When computing this product for the sum of all Fourier components of T^* and v^*, the total heat flux is obtained.

The first right-hand term of Eq. (1) corresponds to the nonlinear contribution of anomalous waves. The sum of the second and third right-hand terms of the equation represents the linear interaction between climatological and anomalous waves (i.e., the modulation of climatological waves by wave anomalies). The values of the total anomalous eddy heat flux and its contributing terms associated with the occurrence of BHs around each grid point are then plotted in the corresponding grid point of a two-dimensional plot as in N11.

d. Extreme polar vortex events

The link between the location of BHs and the occurrence of extreme polar vortex events (major stratospheric warmings and strong polar vortex events) is analyzed in this work. The central date of MSWs is identified by applying the World Meteorological Organization (WMO) criterion (Labitzke 1981). According to this criterion, a MSW is defined by a simultaneous reversal of the zonal-mean zonal wind at 10 hPa in 60°N and a positive zonal-mean temperature difference between 60°N and the pole. Two events are separated by at least 10 days of consecutive westerly winds, corresponding to the radiative relaxation time scale at 10 hPa (Newman and Rosenfield 1997). Stratospheric final warmings are ruled out by requiring 10 days of westerly winds before 30 April and after the occurrence of a warming. According to this criterion, Ayarzagüena et al. (2013) identified a frequency of 5.5 MSWs per decade in the past period in the RCP8.5 run. This value agrees well with the 6.0 events per decade detected in observations of the same period (Charlton and Polvani, 2007). In the future, MSWs show an increase in their frequency with respect to the past (8.3 versus 5.5 events per decade, respectively), but this change is not statistically significant at a 95% confidence level. In fact, the only significant change that is found in the future is a shift in the seasonal distribution of MSWs in winter toward middle and late winter (Ayarzagüena et al. 2013).

Strong polar vortex events (SPVs) are computed based on the northern annular mode (NAM), defined as the first empirical orthogonal function (EOF) of the monthly mean 10-hPa geopotential height anomalies in winter (NDJFM) poleward of 20°N (Baldwin and Dunkerton 2001). The daily NAM index is calculated by projecting the 8-day low-pass-filtered 10-hPa geopotential height (Z) anomalies onto the NAM pattern (N11). SPVs are identified when the NAM index exceeds +1.5 standard deviation, so that the number of events is close to that of MSWs in the past. A further verification has been done to ensure that SPVs are related to values of zonal mean zonal wind at 60°N and 10 hPa stronger or very close to the critical stratospheric velocity at this latitude for the propagation of wavenumber-1 (WN1) Rossby waves ($\sim$30 m s^{-1}) (Andrews et al. 1987).

Since McLandress and Shepherd (2009) have suggested that a relative criterion based on the NAM index is more suitable for the analysis of future MSWs than an absolute one, we have repeated the analysis about the location of BHs prior to MSWs but, in this case, identifying the extreme weak polar vortex events based on the NAM index. Although the change in the frequency of MSWs is not statistically significant in any of both criteria (WMO and relative), the results for this geographical analysis show some mismatch. In spite of this, as our analysis is purely focused on the dynamics and we are not interested in a frequency analysis, we prefer to keep the criterion based on the reversal of the wind for the identification of MSWs due to its dynamical implications, namely that it determines whether PWs propagate or not into the middle stratosphere [in agreement with Bell et al. (2010)].

e. Statistical tests

In this study different two-tailed Student's t tests (with one or two samples of independent events) are used to compute the statistical significance of the results and provide robustness to the conclusions. To compute the statistical significance of anomalies of different fields in

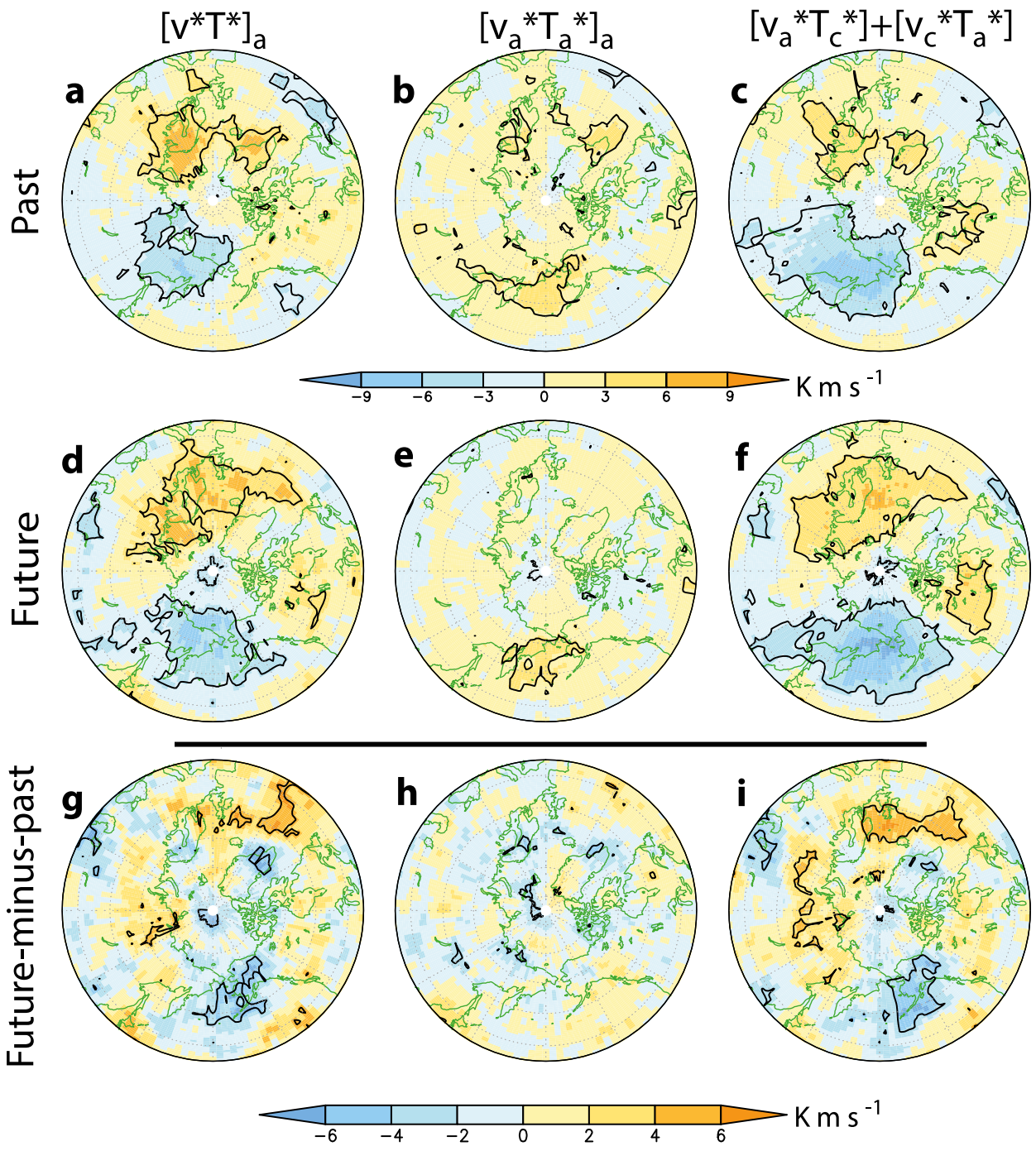

FIG. 1. (a) Area-averaged anomalous eddy heat flux $[v^*T^*]_a$ poleward of 45°N at 100 hPa for the −2 to +7 days around the peak of BHs, composited for the BH events observed in the vicinity of a given location in the past period of the EMAC RCP8.5 run. (b),(c) As in (a), but for the two contributors of $[v^*T^*]_a$: the nonlinear term $[v_a^*T_a^*]_a$ and the interaction term $[v_c^*T_a^*] + [v_a^*T_c^*]$, respectively. (d)–(f) As in (a)–(c), respectively, but for the future period. (g)–(i) As in (a)–(c), respectively, but for the difference of future minus past. Shading interval in (a)–(f) is 3 K m s $^{-1}$ and in (g)–(i) is 2 K m s^{-1}. Contours indicate the regions with statistically significant values at a 95% confidence level (*t* test). The plots are displayed in stereographic projection oriented 180°.

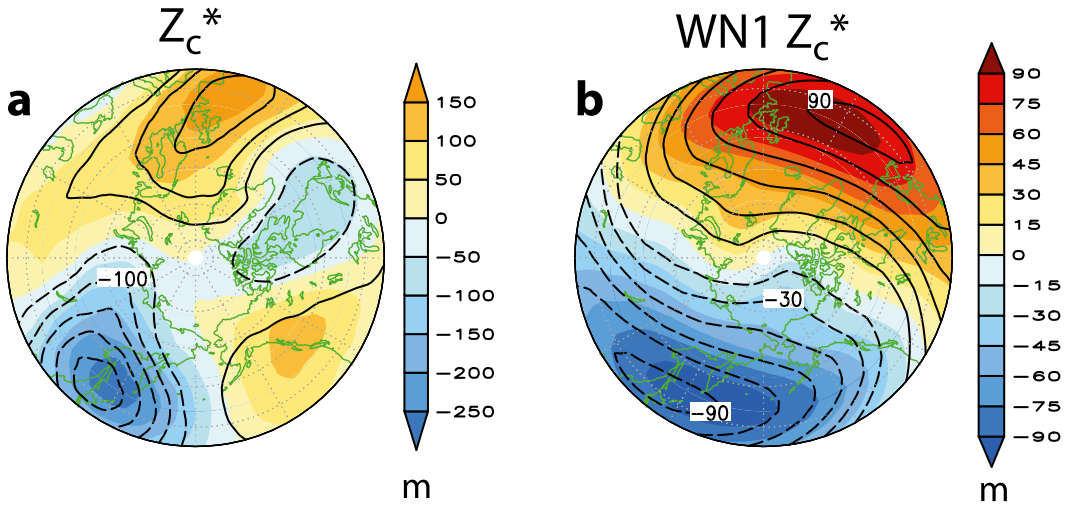

FIG. 2. (a) Deviation of the climatological mean of geopotential height at 250 hPa from its zonal mean in the past (contours; interval: 50 m) and future (shading; interval: 50 m) of the RCP8.5 run. (b) As in (a), but associated only with stationary WN1 (shading and contour intervals are 15 m).

a composite map, a one-sample Student's t test is applied. In this test, we set as null hypothesis (H_0) the anomalies to be zero. Thus, the rejection of H_0 will imply the composited anomalies to be statistically significantly different from zero. In contrast, in future-minus-past difference plots, a two-sample Student's t test was used to determine whether these differences are statistically significant. In this case, the null hypothesis is the equality of the means of the future and past periods and since the sum of the number of events in both periods is higher than 30, the null distribution of Student's t distribution coincides with the typified normal distribution (Wilks 2011).

3. Results

a. *Effects of the location of BHs on the upward propagation of PW activity*

As a first step, the ability of EMAC to reproduce the effects of the location of BHs on the upward wave propagation in the recent past has been assessed and compared with the results from the Japanese 25-year Reanalysis Project (JRA-25) in N11. The first row of Fig. 1 illustrates the anomalies of the area-averaged 100-hPa eddy heat flux poleward of 45°N for the period from −2 to +7 days around the peak time of BHs for the recent past in the EMAC RCP8.5 run as a function of location. The same is shown for the two contributing terms to the total anomalies [Eq. (1)]. The time window was selected based on the evolution of the anomalous eddy heat flux associated with the occurrence of BHs around two specific grid points. These two grid points are located over the western Pacific (68°N, 174°E) and northern Eurasia (71°N, 37°E), where, according to N11, BHs have a strong and opposite influence on the upward wave propagation. The anomalous heat flux is strongest between −2 and +7 days around the occurrence of BHs (not shown).

Figure 1a shows that whereas BHs over the western North Pacific and northeastern Asia tend to reduce the upward propagation of PW, those over the Euro-Atlantic sector lead to an enhancement of upward-propagating wave activity. This agrees well with previous results (e.g., Castanheira and Barriopedro 2010; Nishii et al. 2010; N11). More specifically, the interaction term (Fig. 1c) is the most important contributor to $[v^*T^*]_a$, in EMAC. This is consistent with the spatial coincidence of BH-associated positive or negative anomalies of heat flux and climatological ridges or troughs, respectively (cf. Figs. 1a and 2).

There is also a good agreement between EMAC results and N11 in the spatial pattern of influence of BHs on the eddy heat flux, since the locations of BHs with associated statistically significantly positive or negative anomalies of eddy heat flux are similar to those observed in reanalysis data (cf. Figs. 5a,d,g of N11). Additionally, the magnitudes of the anomalous eddy heat flux and its two contributing terms are within an order of magnitude of the values shown in N11. The only evident discrepancy is the smaller extension of the regions of BHs with associated statistically significant values of heat flux over the Euro-Atlantic sector and eastern Asia in EMAC, which also appears even when considering 30 events for each grid point as in N11.

In the future, there are no major changes in the main locations of BHs with associated enhancement or reduction of $[v^*T^*]_a$ (Fig. 1d). However, some geographical modifications in the main pattern are detected, particularly, in the latitude band between 55° and 70°N, where BHs have the highest influence on the wave activity. The wave-influencing

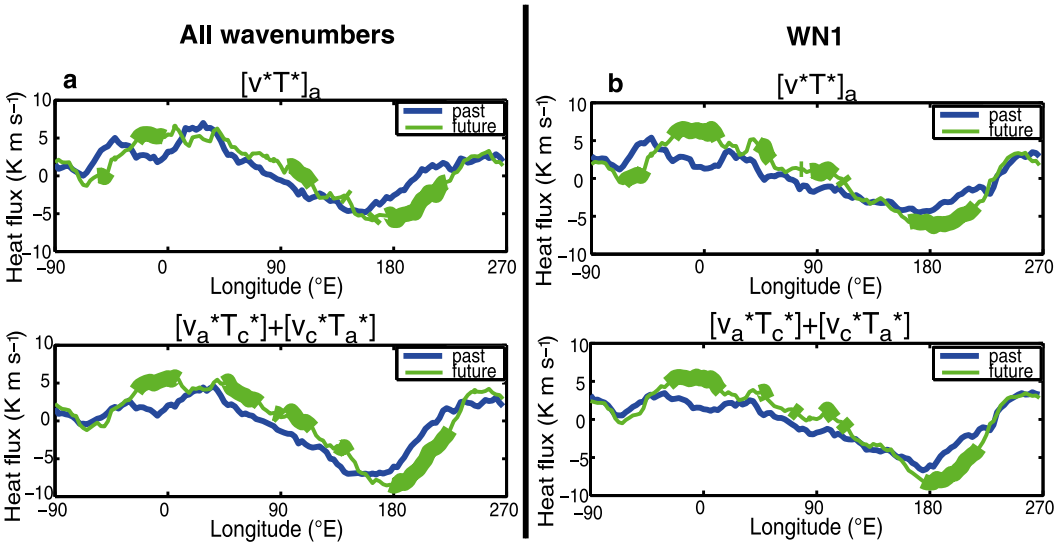

FIG. 3. (a) (top) Area-averaged anomalous eddy heat flux $[v^*T^*]_a$ poleward of 45°N at 100 hPa and (bottom) its interaction term $[v_c^*T_a^*] + [v_a^*T_c^*]$ for the −2 to +7 days around the peak of BHs, composited for the BH events observed in the 55°–70°N latitude band in the past (blue line) and the future (green line) periods of the RCP8.5 run. (b) As in (a), but associated only with WN1. The thickened lines denote that the future values are statistically significantly different from the past ones at a 95% confidence level (*t* test).

BHs over the North Pacific shift eastward and those over the Euro-Atlantic sector occupy a more extended area in the future, particularly over the eastern edge of the region (Figs. 1 and 3a). The shift over the Pacific region is also represented by the significantly positive future-minus-past differences over Siberia and the negative ones over Alaska, particularly in the interaction term (Fig. 1i). It is also statistically significant over the latitude band of 55°–70°N (Fig. 3a). The larger extension of the regions of wave-influencing BHs in the Euro-Atlantic area is also evident in the statistically significantly positive future-minus-past differences on both sides of that sector (Figs. 1g,i). At the latitude band of 55°–70°N the larger future extension is clear on the eastern side (Fig. 3a). In addition, the interaction term intensifies in the future with statistically significantly stronger values over the regions with significant positive and negative values of this term (Figs. 1 and 3a). This result represents a more effective interaction between the wave anomalies related to BHs and the climatological waves.

Figure 4 shows the same variables as Fig. 1 but only for the WN1 component. In both past and future, the contribution of WN1 to the total fields is the largest, particularly for the interaction term. This is explained by the spatial coincidence between the distribution of BH-associated positive or negative heat flux anomalies and climatological ridges or troughs in the WN1 pattern (compare Figs. 1a and 4a with Fig. 2b). All these features agree well with N11.

In the future period, the changes in the WN1 component strongly resemble those found in the total eddy heat flux field: the increasing magnitude of the interaction term, the eastward shift of the pattern in the North Pacific and the larger extension of the influence sector over Eurasia, particularly eastward. Additionally, Fig. 4 shows an intensification of $[v^*T^*]_a$ associated with WN1 in the future. These future changes are statistically significant (Figs. 4g–i and 3b).

We have so far focused on the analysis of the WN1 component of the wave activity since it is the predominant one, showing the most significant future changes that account for most of those detected in the overall wave activity. Nevertheless, it should be pointed out that while BHs over the western North Pacific and eastern Asia are characterized by a suppression of upward wave activity, BHs over the eastern Pacific and Alaska tend to enhance the wavenumber-2 (WN2) component of wave activity (not shown). This positive contribution of the WN2 eddy heat flux explains the disagreement in the sign between the total $[v^*T^*]_a$ and the WN1 component over Alaska (Fig. 1a versus Fig. 4d) and it is consistent with previous studies showing that split MSWs are usually preceded by BHs over that region (e.g., Martius et al. 2009).

b. *Influence of the location of BHs on polar stratospheric variability*

As the location of BHs critically influences the anomalous meridional heat flux and, thus, the upward propagation of PW, there should also be a geographically dependent effect of the BHs on the polar stratospheric temperature (e.g., Newman et al. 2001). To verify this, we have analyzed the changes in the stratospheric

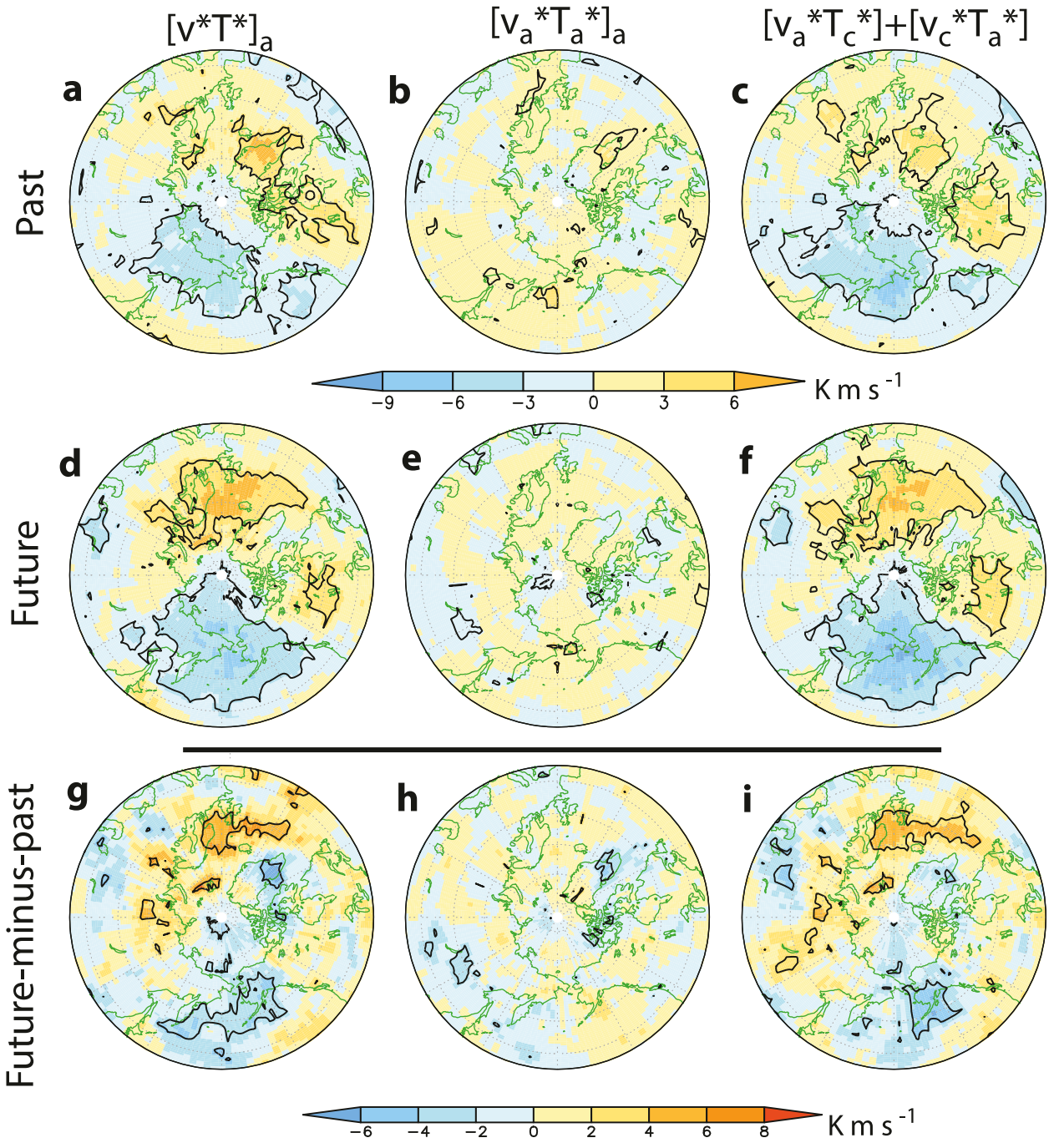

FIG. 4. As in Fig. 1, but only for WN1.

temperature poleward of 70°N. Following the methodology of N11, the tendency of the anomalous polar temperature at 10 hPa during the occurrence of BHs has been computed (Fig. 5). This tendency corresponds to the difference in the anomalous temperature between the averaged periods from +5 to +14 days and from −10 to −1 days of the peak time of BHs.

Figure 5 demonstrates that the effect of the geographical location of BHs on the polar stratospheric temperatures is consistent with its effect on the PW propagation in both periods of study. The BHs that lead to an enhancement of wave activity are associated with a subsequent warming of the polar stratosphere. The opposite occurs for the BHs that are responsible for

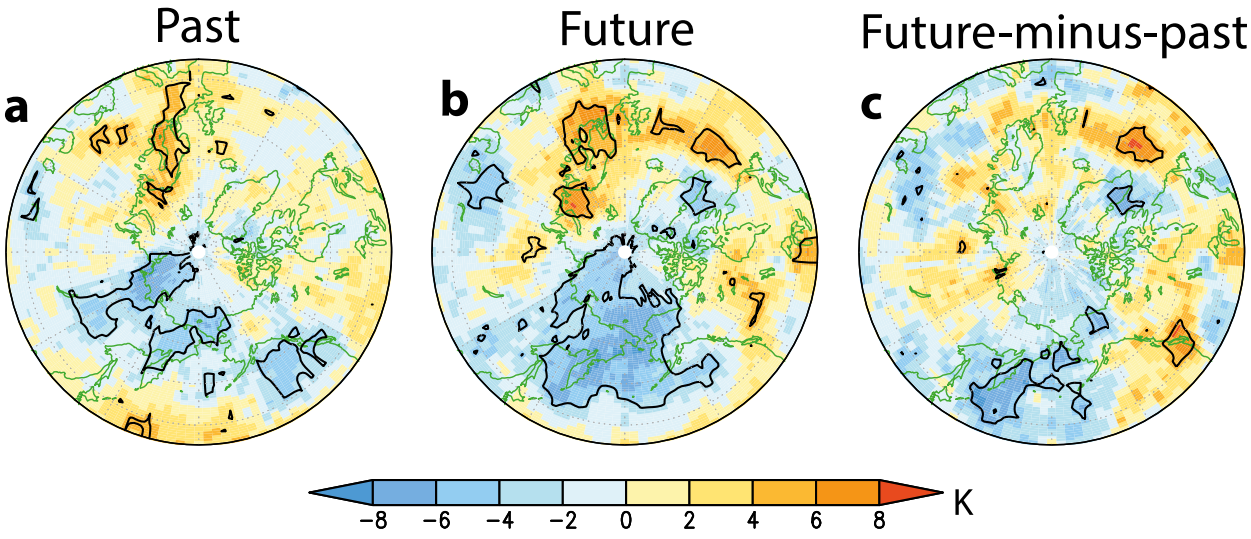

FIG. 5. Tendency in the anomalous temperature poleward of 70°N at 10 hPa associated with the occurrence of BHs around each grid point. The tendency is computed as the difference between +5 to +14 days after the peak of BHs and −10 to −1 days before their peak for the (a) past and (b) future period of the RCP8.5 run. Shading interval: 2 K. Contours indicate the regions with statistically significant values at a 95% confidence level (*t* test).

a suppression of wave activity. An aspect to highlight is that the regions with statistically significant values are larger over the eastern Asia-Pacific region than over the Euro-Atlantic sector in both periods. The asymmetry between the two sectors is also reflected in the plots of anomalous heat flux, particularly in the WN1 component, and was detected by N11 in reanalysis data. This could be related to the fact that BHs over the North Pacific usually originate in the eastern part and retrograde toward eastern Asia, leading to a more prolonged influence on the WN1 wave propagation and the polar stratosphere than BHs over Eurasia (Takaya and Nakamura 2005; N11).

The future changes in the geographically dependent response of the polar stratospheric temperature are similar to those found for the heat flux. In particular, BHs with influence on stratospheric temperature occupy larger areas in the future than in the past. This change is statistically significant (Fig. 5c) and is presumably related to the future intensification of the interaction between climatological waves and BH-associated wave anomalies.

The relationship between the geographical location of BHs and their effects on the polar stratosphere temperature anomalies suggests that BHs would also tend to appear in preferred regions preceding extreme polar vortex events. This is confirmed by Fig. 6, which shows the fraction of BHs (%) around each grid point in the 10 days preceding the central date of weak or strong vortex events (MSWs and SPVs, respectively). The values of this fraction, however, are not very large, particularly for the past MSWs, because of the low probability of extreme polar vortex events with respect to the total number of days in each period of study and the particular restrictions imposed in the identification of BHs (separation of events).

In the case of past MSWs, the geographical distribution of BHs preceding MSWs agrees well with that of BHs enhancing planetary wave activity (Fig. 6a). However, in the future, BHs prior to MSWs tend to be more delocalized and a higher fraction of BHs is found in most regions (particularly over the Atlantic and Eurasia) compared to the past (Fig. 6b). Different reasons could be behind this delocalization. One might be the increase in the frequency of MSWs, although it is not statistically significant. In fact, when selecting extremely weak polar vortex events based on the NAM index (with a threshold of −2 standard deviation and the same number of events in both periods), BHs are still found in a larger area over Eurasia in the future than in the past, but the delocalization is reduced (not shown).

Another explanation for this delocalization might be a future decrease in the frequency of BHs [already shown by some studies from phase 5 of the Coupled Model Intercomparison Project (CMIP5) such as Dunn-Sigouin and Son (2013) or Masato et al. (2013)], because we fix the same number of events around each grid point for both periods of study. Thus, some anticyclonic anomalies that are not blockings according to the definitions used by the cited studies might be included and have a weak effect on the upper-tropospheric wave activity and the polar stratosphere. However, as already shown, the selected future BHs lead, in general,

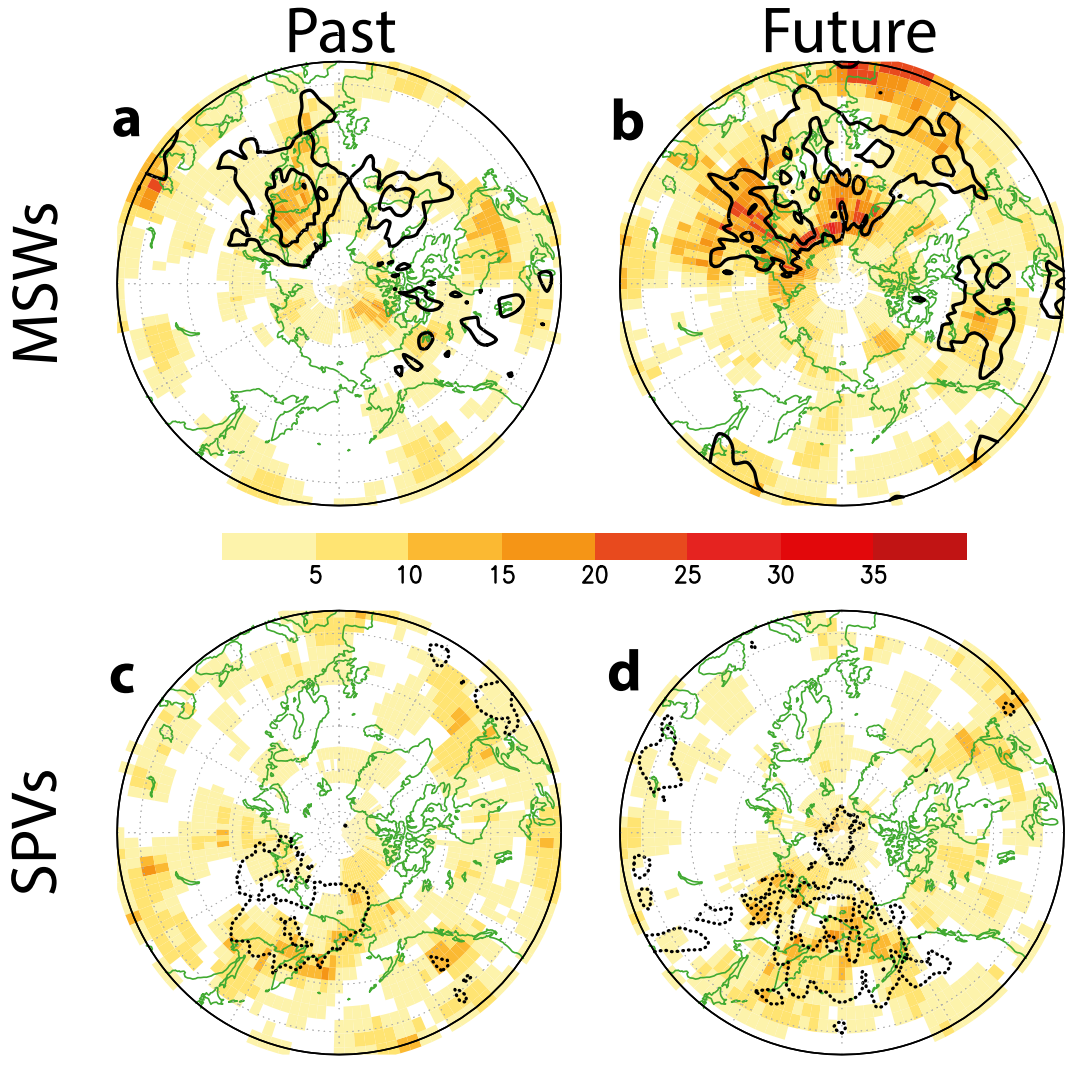

FIG. 6. Fraction (%) of BHs out of the total 20 BHs around each grid point that take place in the 10 days preceding the central date of (a) past MSWs, (b) future MSWs, (c) past SPVs, and (d) future SPVs in the RCP8.5 simulation. Solid (dotted) lined in MSWs (SPVs) plots denote positive (negative) values of anomalous heat flux higher (lower) than 3 (−3) K m s^{-1} shown in Figs. 1a and 1d for the past and future period in shading, respectively.

to stronger anomalies of heat flux of both signs depending on the location and in a more effective influence of BHs on the polar stratospheric temperature. In fact, the higher number of future BHs over the Atlantic and Eurasia prior to MSWs can be related to a weaker polar vortex in the future and a stronger upward wave activity associated with BHs over that area. Both features are consistent with each other. The stronger wave activity is reflected in the intensification of the anomalous heat flux as a result of a strengthening of the WN1 component of the interaction term of the eddy heat flux associated with the onset of BHs (Figs. 1 and 4) and in the farther extension of strong anticyclonic anomalies in these regions that will be shown in section 4. The increasing importance of the WN1 interaction term prior to MSWs is also verified in Fig. 7, where the evolution of the WN1 component of the anomalous eddy heat flux and its contributing terms around the occurrence of MSWs is shown. It can be seen that the interaction term becomes statistically predominant in the future before and during the peak of the anomalous WN1 wave activity associated with MSWs. A similar feature lacks in the case of the WN2 component of the interaction term (not shown). In addition, in February an increase in the fraction of BHs out of the total 20 BHs around each grid point over the Atlantic and Eurasia has been identified (not shown), which is consistent with the month with the highest future increase in the number of BHs in the RCP8.5 run (Ayarzagüena et al. 2013).

Another remark about future changes in the position of BHs prior to MSWs concerns the location of the BH

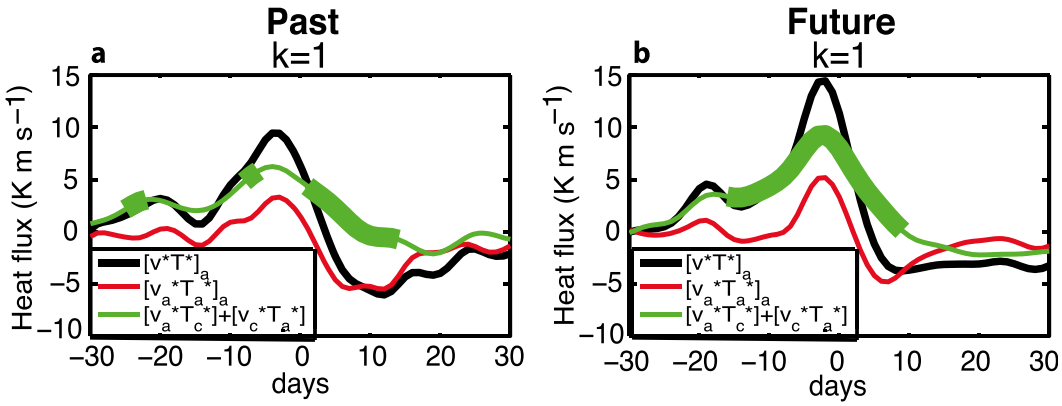

FIG. 7. Composite daily heat flux anomaly poleward of 45°N (K m s^{-1}) at 100 hPa from 30 days before to 30 days after the central date of MSWs for the (a) past and (b) future period of the RCP8.5 run for the WN1 component. The different lines indicate total anomalies (black line) and its different contributions (colored lines): the nonlinear term $[v_a^* T_a^*]_a$ and the interaction term $[v_c^* T_a^*] + [v_a^* T_c^*]$. Thickened lines indicate when the linear term is statistically significant different from the nonlinear one.

maximum over Eurasia. Whereas it is located over Scandinavia in the past, the future maximum is located over Ural Mountains. This eastward shift is consistent with the farther eastward extension of BHs affecting wave activity.

Concerning the SPVs, the past distribution of BHs also agrees well with the results for the eddy heat flux anomalies and with those of N11; that is, there is a clustering of BHs over the North Pacific preceding the occurrence of SPVs in both periods of study (Figs. 6c,d). In the future, BHs preceding SPVs remain mainly localized over eastern Asia and the northwestern Pacific, the main region with a destructive interaction between wave anomalies and the climatological WN1 wave (Fig. 6d). However, consistent with the eastward shift of the interaction term noted above (Fig. 1i), their probability of appearance decreases over eastern Asia.

4. Discussion

In section 3 the ability of EMAC to reproduce the effects of the location of BHs on the upward propagating PW activity and on the polar stratospheric temperature in wintertime as seen in reanalysis (N11) was shown. While no major future changes in the influence pattern of BHs on the upward PW propagation were detected, geographical variations in the main pattern over the Pacific and Euro-Atlantic regions and the intensification of the WN1 component of the interaction between climatological waves and wave anomalies that accounts for most of the changes in the wave activity were identified. In this section, we will discuss the possible causes for these changes and the robustness of the future signal.

a. Possible explanations for the future changes in the response of the wave activity to the location of BHs

In Fig. 8, the mean geopotential height amplitude of the BHs around each grid point in their peak time is compared in the past and future to link possible variations in the properties of BHs to the changes in the geographically dependent response of PW activity to BHs. In the past, the BHs located over the North Pacific and the western Atlantic were associated with the largest anticyclonic anomalies (Fig. 8a). In the future, an eastward displacement of the centers of maximum anomalies (Fig. 8b) occurs in both sectors, visible by the negative (positive) values on the west (east) side of the basins in the difference plot (Fig. 8c). Thus, the eastward shift of the pattern of influence of BHs on the upward PW propagation coincides with a shift of the BH amplitude. Apart from this common shift, we also see specific changes in each sector. Over the Pacific, the BHs get, in general, stronger in the future, particularly east of the date line. In the Euro-Atlantic sector, strong anomalies extend farther downstream, indicating an intensification of the BH amplitude over Eurasia. As mentioned in section 3b, this also explains at least partially the delocalization of the future BHs preceding MSWs. The region with strong anticyclonic anomalies over the Euro-Atlantic area is broader in the future, which favors a larger area with an effective positive modulation of the climatological waves by BHs. Future changes of BHs over the Euro-Atlantic sector in EMAC are similar to those described by Sillmann and Croci-Maspoli (2009) or de Vries et al. (2013). Both studies found an eastward shift of the blockings in winter in the future when analyzing ECHAM5 simulations. Sillmann

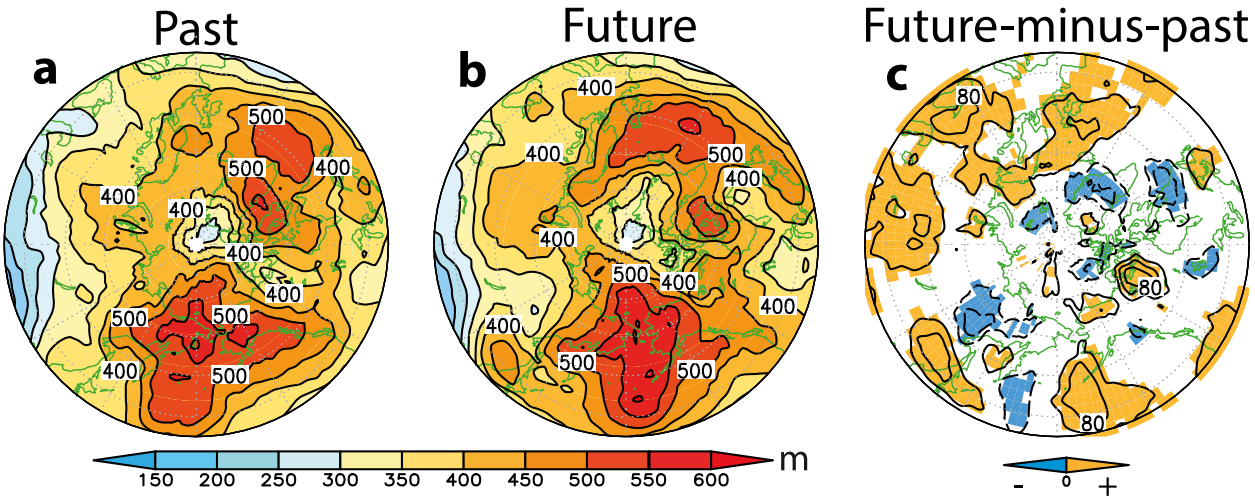

FIG. 8. (a) Composite of low-pass-filtered daily anomalies of geopotential height at 250 hPa for the day of the peak time of the 20 BHs identified around a given grid point in winter in the past period of the RCP8.5 run. (b) As in (a), but for the future period of the same run. (c) Future-minus-past difference. Contour intervals: 50 m in (a) and (b) and 40 m in (c). Shading in (c) shows statistically significant values at a 95% confidence level (t test).

and Croci-Maspoli (2009) identified an intensification of the blockings in the area around the British Isles toward the Norwegian Sea as a consequence of this shift. Some CMIP5 studies have also shown a decrease in the frequency of BHs over the Atlantic and an increase over western Russia in the annual mean or in wintertime (Dunn-Sigouin and Son 2013; Masato et al. 2013). This change is present in multimodel annual mean (Dunn-Sigouin and Son 2013) and in half of the models analyzed by Masato et al. (2013) for winter, being the Max Planck Institute Earth System Model, medium resolution (MPI-ESM-MR, a new generation of ECHAM5 and so, belonging to the same atmospheric model family as EMAC), among them. However, in this season, models show some spread in the frequency change over the Euro-Atlantic sector (de Vries et al. 2013; Masato et al. 2013).

De Vries et al. (2013) explained the future farther eastward extension and displacement of the Euro-Atlantic winter blockings by changes in the mean climate, particularly an increased downstream variance, due to a stronger and more eastward extending future upper-tropospheric jet. They found that because of this increase in variability, Rossby wave breaking takes place farther eastward, favoring the more eastward occurrence of blockings. In EMAC, similar future intensification and larger extension of the mean jet are detected in the Atlantic area (Fig. 9a). The increase in zonal wind is located approximately over the jet and it is stronger in the entrance and the exit regions of the jet than in its core. Toward Europe, the wind increase in the exit of the jet denotes a farther eastward extension of the future jet. This explains the higher amplitude of the BHs over Eurasia in the future, since these changes in the background state favor the occurrence of strong anticyclonic systems farther eastward.

In addition, variations in the climatological eddy geopotential height (Z_c^*) at 250 hPa (i.e., the climatological deviation of Z from the zonal mean) are also identified in the future (Figs. 2 and 9c). In Fig. 9c, we show for both periods the wintertime Z_c^* at 250 hPa averaged between 40° and 60°N together with the composite amplitude of BHs in that latitude band. The selected latitude band corresponds to that where Z_c^* shows its maximum values at this level. First, a slight increase in Z_c^* can be seen between approximately 50° and 90°E, a longitude range where the BH amplitude is also increasing. Second, an eastward shift of Z_c^*, particularly over eastern Asia–North Pacific is found, coinciding with a similar shift and increase in the BH amplitude distribution. Hence, Z_c^* decreases in a 60° longitude sector centered at the date line. These changes can also be identified in Fig. 2a. As the interference between climatological and BH-associated anomalous waves depends partly on the relative phase of the climatological and anomalous waves, a shift of Z_c^* also affects the pattern of the interaction term, resulting in an eastward shift of the interaction term.

A future change in the upper-tropospheric jet is also identified over the eastern Asia–Pacific area (Fig. 9a). The jet shifts northeastward, as represented by positive future-minus-past differences of the zonal wind at 250 hPa at the northeastern edge of the Asian–Pacific jet and negative differences at its southwestern part (Fig. 9a). This shift coincides with a significant future

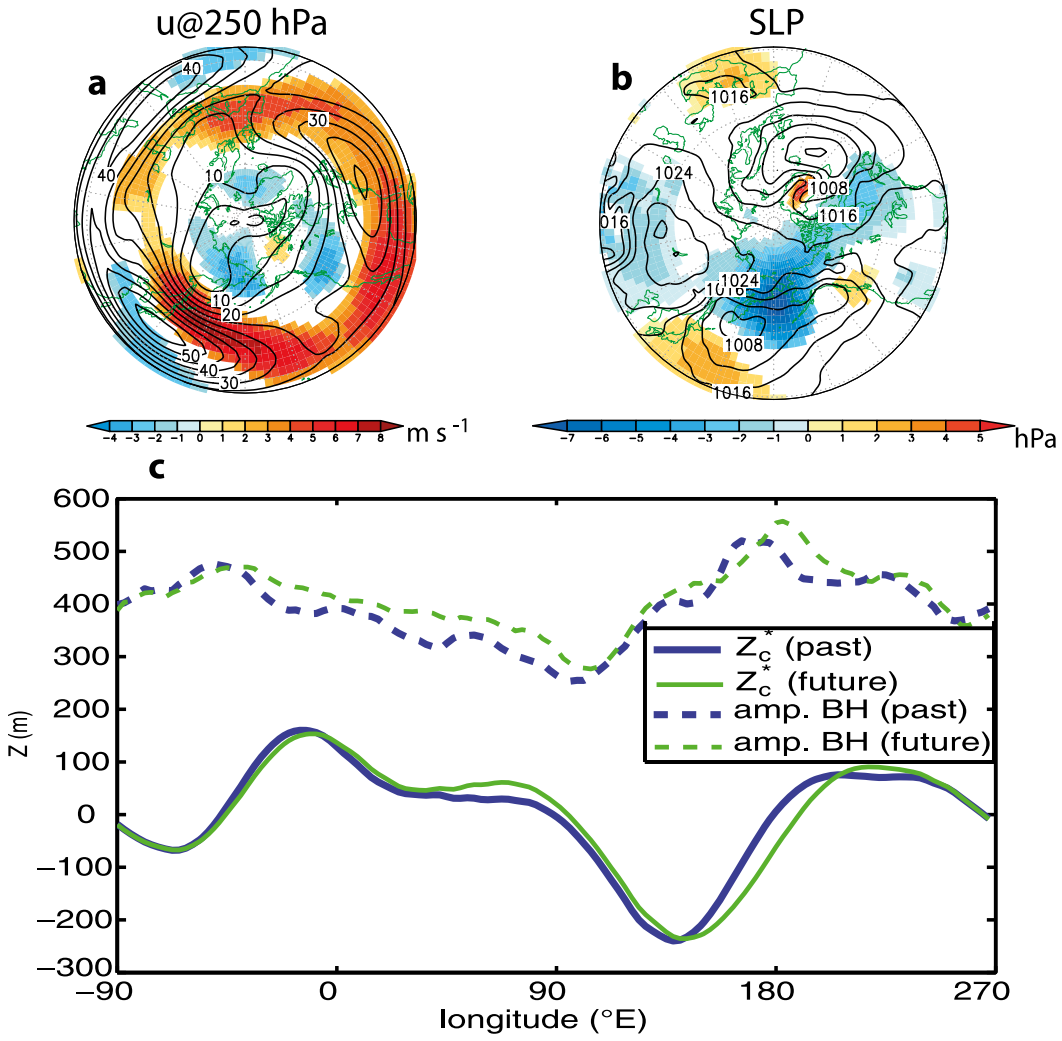

FIG. 9. (a) Climatological zonal wind at 250 hPa for the extended winter (NDJFM) in the past period of the RCP8.5 run (contours; interval: 5 m s^{-1}) and statistically significant future-minus-past differences of this climatology at a 95% confidence level (shading; interval: 1 m s^{-1}). (b) As in (a), but for the mean sea level pressure (contour interval: 4 hPa and shading interval: 1 hPa). (c) Wintertime climatological eddy geopotential height at 250 hPa averaged between 40° and 60°N (m) for the past (blue solid line) and the future (green solid line) and composite of the geopotential height anomalies (m) associated with the 20 BHs in each grid point and averaged between 40° and 60°N for the past (blue dashed line) and the future (green dashed line).

change in the Aleutian low, which strengthens and moves northeastward (Fig. 9b). It is responsible for the eastward displacement of the pattern of influence of BHs on the wave activity. The strengthening of the Aleutian low leads to an intensification of the stationary WN1 wave (e.g., Garfinkel et al. 2010), identified in Fig. 2b. Previous studies by Ayarzagüena et al. (2013) and Oberländer et al. (2013) found that GHG-induced tropical SST changes were responsible for the enhancement of future WN1 wave activity in winter. The mechanism involved in the WN1 amplification could be similar to that leading to the stratospheric response to the El Niño phenomenon, as the response of the prescribed SSTs in our run to global warming resembles the El Niño pattern over the equatorial Pacific (not shown). Additionally, we have found changes in the basic state similar to the extratropical response to El Niño: deepening and northeastward shift of the Aleutian low (Horel and Wallace 1981). Finally, some authors such as Taguchi and Hartmann (2006), Ineson and Scaife (2009), and Garfinkel et al. (2010) have found an amplification of the stationary WN1 wave activity as a result of the intensification of the Aleutian low related to El Niño events.

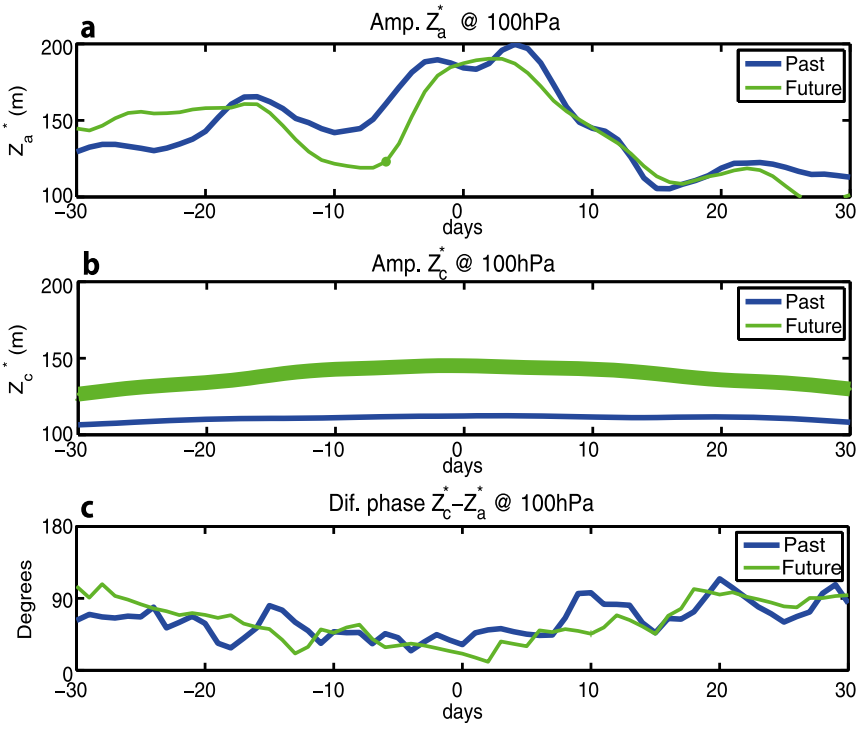

FIG. 10. (a) Composite during MSWs of the amplitude of the anomalous WN1 geopotential height (Z_a^*, m) at 60°N and 100 hPa for the past (blue line) and the future (green line) of the RCP8.5 run. (b) As in (a), but for the climatological stationary WN1 wave of the same variable (Z_c^*). (c) Composite of the phase difference between the WN1 Z_a^* and Z_c^* (degrees). The thickened lines denote that the future values are statistically significant different from the past ones at a 95% confidence level (t test).

As expected, the intensification of the WN1 stationary wave is also identified at 100 hPa, where we have detected the future intensification of WN1 heat flux anomalies, particularly in the interaction term, in section 3 (Figs. 4 and 7). Since the intensity of the interaction between climatological and anomalous waves depends not only on the amplitude of the climatological wave, but also on the amplitude of the anomalous wave and the phase difference between them, it is important to determine how the possible changes in these three factors contribute to the strengthening of the interaction term of the eddy heat flux. Therefore we have isolated the effects of each factor during the occurrence of MSWs, which are triggered by strong injection of tropospheric wave activity. Figure 10 shows the evolution of the mean amplitudes of the anomalous and the climatological stationary waves of WN1 Z^* at 60°N and 100 hPa and the phase difference between them during the period from −30 to +30 days before and after the occurrence of these events in the past and future. From this analysis, one can deduce that the future intensification of the WN1 interaction term in section 3 (more exactly in this case in Fig. 7) comes from the amplification of the stationary WN1 wave, as it is the only factor that shows a statistically significant change in the future. This implies that it is mainly the change in the climatological mean state, rather than the variability about that state, that dominates.

It is necessary to note that although most climate models project an El Niño–like pattern in the future, a few atmosphere–ocean coupled GCMs (AOGCMs) do not show this pattern (Collins et al. 2014). As the future intensification of WN1 wave activity could be dependent on this SST response, it could be absent in those models that do not include the strong signal over the tropical Pacific in the future.

b. *Robustness of the future signal*

To test the robustness of our previous results deduced for an extreme climate change scenario (RCP8.5), we have repeated the analysis for another simulation under a weaker future scenario (RCP4.5). Figure 11 shows the results for the response of the PW upward propagation to the location of BHs for the RCP4.5 scenario. In the past, the main regions with BHs influencing the wave propagation are comparable to those of the RCP8.5 run (Figs. 11a–c versus Figs. 1a–c), which is consistent with

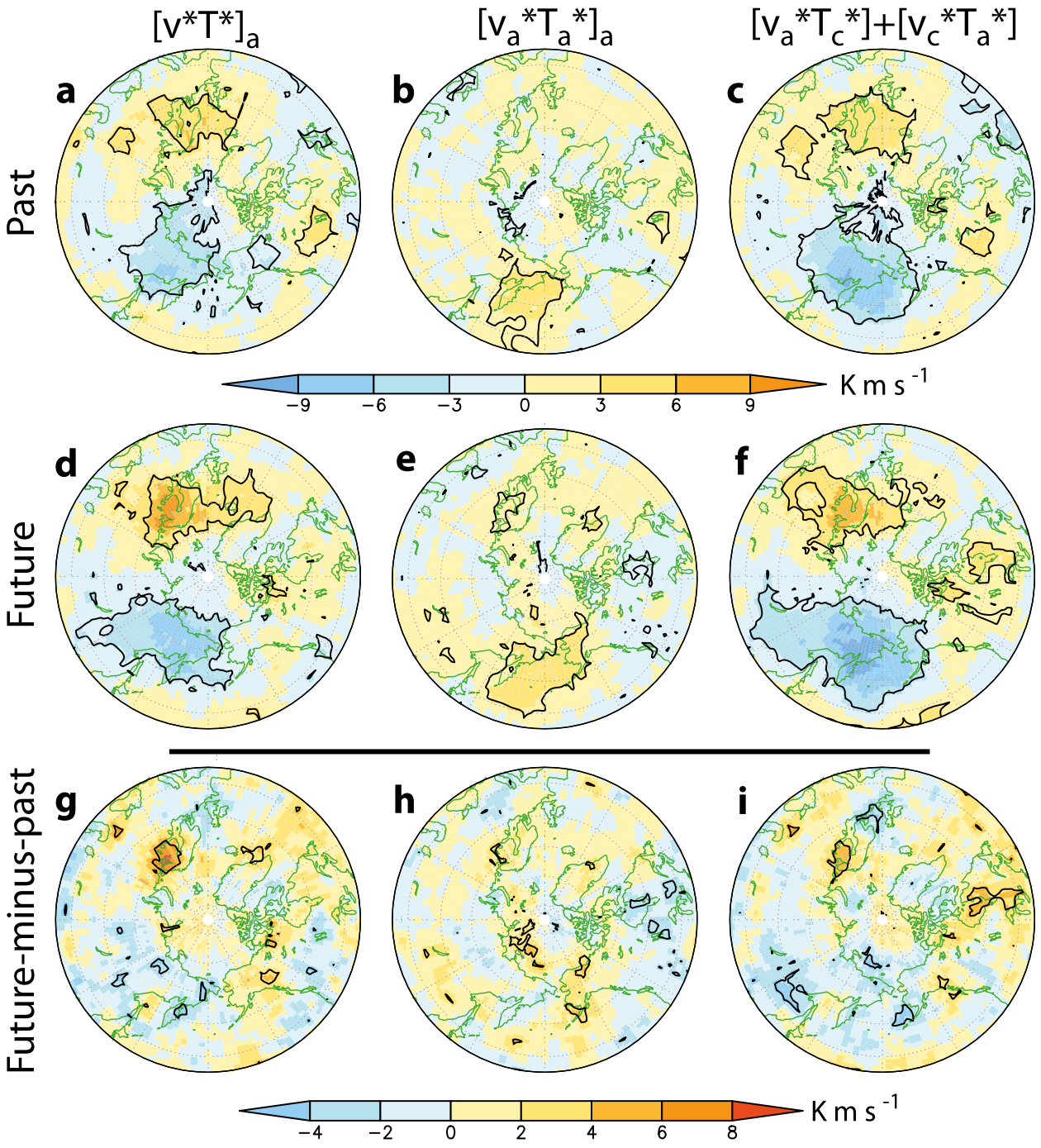

FIG. 11. As in Fig. 1, but for the RCP4.5 run.

the similarity in forcings of both runs in the past. In particular, the pattern of influence of BHs on the interaction term of the eddy heat flux is comparable. This is important since it has been shown that BHs mainly produce the modulation of the PW activity through the interaction of the anomalous waves associated with these structures and the climatological waves. Nevertheless, some differences are found, most of them concerning the $[v_a^* T_a^*]_a$ term due to internal variability of the model (Fig. 11b).

On the other hand, when comparing the past and the future of the RCP4.5 run, similarities in the future changing pattern of BH influence on the upward PW propagation are identified with respect to those detected

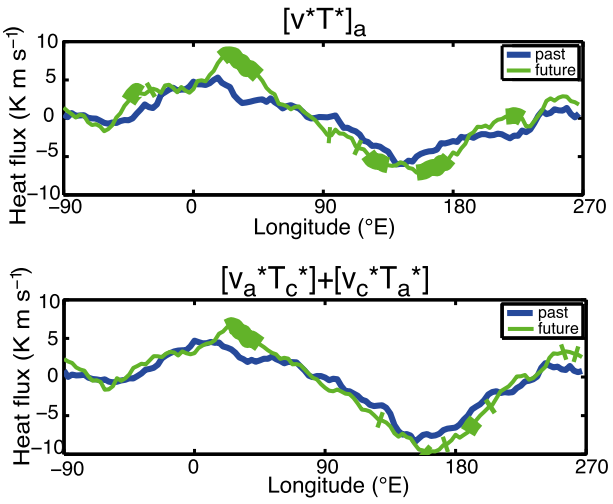

FIG. 12. As in Fig. 3a, but for the RCP4.5 run.

in the RCP8.5 run. However, these common changes between both runs only concern the interaction term and are much weaker in the RCP4.5 run than in the RCP8.5 one that the statistical significance of the RCP4.5 changes is very weak (Figs. 11g–i). The eastward shift over the Pacific and the larger eastward extension over the Atlantic in RCP4.5 are also identified in the interaction term (Figs. 11c,f) but, for instance, the former is not obvious in the total anomalous eddy heat flux plot (Figs. 11a,d). This is because of the positive contribution of the nonlinear term that is not reduced in the future in the RCP4.5 run in contrast to the RCP8.5 one (Figs. 11b, e,h), but even intensifies and extends farther eastward over the Pacific sector (although not statistically significantly). For a more detailed analysis of the robustness of the signal and because of the noise in Fig. 11, we have repeated the same analysis of the heat flux associated with the BHs over the latitude band 55°–70°N, where the BHs have the strongest influence on the wave activity (Fig. 12). The eastward shift of the pattern over the Pacific is evident in the future shift in the peak of the negative values of heat flux around 160°E in the total field and the interaction term. The farther eastward extension of BHs with significant influence on the heat flux over Eurasia is clearly indicated by the stronger values of heat flux in the region between 10° and 50°E. In both plots the stronger peaks of heat flux in the Euro-Atlantic and Pacific sectors in the future highlight the intensification of the interaction term.

Please note the following two comments on the robustness of the future changes. First, the upper tropospheric jet in the RCP4.5 run shows a weaker but similar change in the future to that in the RCP8.5 simulation and affects the response of the BH amplitude to future climate change in a similar way. Second, because of the apparent large internal variability of the model, we have repeated the analysis of the future changes in both RCP4.5 and RCP8.5 runs, but with a common past period corresponding to the average of both experiments considered as two ensemble members. In this second analysis, the regions with statistically significant future-minus-past differences of the total anomalous heat flux and interaction term are almost coincident, when considering 40 or 80 years for the past period. Thus, the results of this second analysis confirm the conclusions derived from the comparison of 40-yr periods of data.

In summary, the future changes in the pattern of BH influence on the upward propagating PW activity detected in the RCP8.5 run also appear in the RCP4.5 run, but they are weaker because of the higher intensity of the climate change signal in RCP8.5 than in RCP4.5. Among others effects, this involves stronger GHG-induced SST changes that seem to play a relevant role in future changes in the tropospheric dynamical forcing as revealed by studies using different models (e.g., Oman et al. 2009; Oberländer et al. 2013).

5. Summary and conclusions

In this study we have examined possible future changes in the response of the wave activity to the location of BHs and their effects on stratospheric variability in transient simulations of the period 1960–2100 carried out with EMAC CCM. While some recent studies have already analyzed this response for the recent past by using reanalysis data and model simulations (Martius et al. 2009; Orsolini et al. 2009; Castanheira and Barriopedro 2010; Nishii et al. 2010; Woollings et al. 2010; N11; Bancalà et al. 2012; Vial et al. 2013), none has explored this relationship in the future yet, as far as we know.

First, it has been verified that EMAC is able to reproduce qualitatively well the geographical dependence of the BH influence on PW injection into the stratosphere and on stratospheric variability. In particular, by applying the same methodology as N11, it was shown that whereas BHs over the western Pacific tend to weaken the upward propagation of PWs leading to a strengthening of the polar vortex, the effect of BHs over the Euro-Atlantic sector on PWs is the opposite, favoring the occurrence of MSWs. These results are consistent with N11. It was found that the modulation of the PW activity by BHs is mainly achieved through the interaction of the wave anomalies associated with these structures and the climatological waves.

Although the main results concerning this response of the PW activity to locations of BHs do not change in the future, the following changes have been found:

- The pattern of the influence of the location of BHs on the upward PW propagation shows an eastward shift in the future in the Pacific region and a larger extension in the Euro-Atlantic sector, particularly on the eastern side. The Euro-Atlantic change appears together with a similar change in the distribution of the strongest BHs and is consistent with previous studies that focused on the response of Atlantic blockings to climate change (Sillmann and Croci-Maspoli 2009; de Vries et al. 2013; Masato et al. 2013). Changes in the mean climate and in particular a stronger and more eastward extending upper-tropospheric jet stream in the future are consistent with this change. A shift in the climatological Aleutian low and in upper-tropospheric jet also leads to the variations in the BH-associated wave pattern over the Pacific.
- The WN1 component of the interaction between climatological waves and wave anomalies associated with the occurrence of BHs becomes more important in the future, resulting in a more effective influence of BHs on the polar stratosphere. This enhancement of the WN1 interaction term originates from an amplification of the climatological WN1 wave, probably related to the influence of the GHG-induced changes in tropical SSTs (Ayarzagüena et al. 2013; Oberländer et al. 2013). As the tropical SST response to global warming resembles the El Niño pattern, the mechanism involved in this amplification of the WN1 stationary wave might be similar to that responsible for the extratropical response to the El Niño phenomenon: intensification and northeastward shift of the Aleutian low (Horel and Wallace 1981; Ineson and Scaife 2009).

The described future changes in the response of the wave activity to the location of BHs modify the distribution of BHs preceding extreme polar vortex events. In the case of MSWs, BHs tend to be more delocalized in the future, occupying a broader area over the Euro-Atlantic sector. In this broad area, the region with strong anticyclonic anomalies is extended farther eastward in the future, leading to a larger area of BHs that could enhance upward propagation of wave activity, as it is coincident with the wide ridge of the climatological WN1 of geopotential height. Additionally, a future intensification of the stationary WN1 activity will contribute at least partially to the future weakening of the polar vortex in middle and late winter and the subsequent, but not statistically significant, change in MSW frequency. As for SPVs, future BHs tend to follow the distribution according to the stationary WN1 wave pattern too, being more concentrated over the Pacific region. In contrast to MSWs, the areas with strong anticyclonic anomalies that lead to a negative interference with climatological waves remain confined to the eastern Asia–Pacific area and do not show a larger extension in the future than in the past. Moreover, in both cases of BHs preceding MSWs or SPVs, an eastward shift of the main regions with BHs is identified in the future in agreement with the changes detected in the pattern of BH influence on the wave activity.

The signal of the derived future changes has been shown to be robust for several reasons. First, while no studies have previously focused on future changes in the influence of the BHs on stratospheric variability, the variations in the background state that explain some of the detected changes in this study agree with those identified by other authors (Sillmann and Croci-Maspoli 2009; Woollings 2010; de Vries et al. 2013; Masato et al. 2013). Additionally, similar changes have been observed in two transient EMAC simulations under different future climate change scenarios (RCP8.5 and RCP4.5). However, the future changes were more prominent under the extreme climate change scenario than under the weaker one. Nevertheless, as the exact geographical distribution and other features of BHs depend on the climatological atmospheric circulation and may be affected by model biases (Scaife et al. 2010; Anstey et al. 2013), it is planned to extend this analysis to the output of different models.

Finally, the results of our analysis have contributed to the explanation of future changes in the wintertime polar stratospheric variability, as it was demonstrated how changes in the tropospheric mean state can also lead to modifications in the location of tropospheric precursors of polar stratospheric variability.

Acknowledgments. This work was partially supported by a bilateral research cooperation program between Norway and Germany funded by the Deutsche Akademischer Austausch Dienst (DAAD) and the Research Council of Norway. BA was supported by the Deutsche Forschungsgemeinschaft (DFG) with the research programme SHARP (LA 1025/13-1), JA was supported by the DFG within ISOLAA /LA 1025/17-1), and AK was supported by the DFG within ProSECCO (LA 1025/5-3). The authors thank the North-German Supercomputing Alliance (HLRN) and the ECMWF computing center in Reading for computing time and support. The authors also thank the anonymous reviewers for their helpful suggestions and comments.

REFERENCES

Andrews, D. G., J. R. Holton, and C. B. Leovy, 1987: *Middle Atmosphere Dynamics*. Academic Press, 489 pp.

Anstey, J., and Coauthors, 2013: Multi-model analysis of Northern Hemisphere winter blocking: Model biases and the role of resolution. *J. Geophys. Res. Atmos.,* **118,** 3956–3971, doi:10.1002/jgrd.50231.

Ayarzagüena, B., U. Langematz, S. Meul, S. Oberländer, J. Abalichin, and A. Kubin, 2013: The role of climate change and ozone recovery for the future timing of major stratospheric warmings. *Geophys. Res. Lett.,* **40,** 2460–2465, doi:10.1002/grl.50477.

Baldwin, M. P., and T. J. Dunkerton, 2001: Stratospheric harbingers of anomalous weather regimes. *Science,* **294,** 581–584, doi:10.1126/science.1063315.

Bancalà, S., K. Krüger, and M. Giorgetta, 2012: The preconditioning of major sudden stratospheric warmings. *J. Geophys. Res.,* **117,** D04101, doi:10.1029/2011JD016769.

Bell, C. J., L. J. Gray, and J. Kettleborough, 2010: Changes in Northern Hemisphere stratospheric variability under increased CO_2 concentrations. *Quart. J. Roy. Meteor. Soc.,* **136,** 1181–1190, doi:10.1002/qj.633.

Castanheira, J. M., and D. Barriopedro, 2010: Dynamical connection between tropospheric blockings and stratospheric polar vortex. *Geophys. Res. Lett.,* **37,** L13809, doi:10.1029/2010GL043819.

Charlton, A. J., and L. M. Polvani, 2007: A new look at stratospheric sudden warmings. Part I: Climatology and modeling benchmarks. *J. Climate,* **20,** 449–469, doi:10.1175/JCLI3996.1.

Collins, M., and Coauthors, 2014: Long-term climate change: Projections, commitments and irreversibility. *Climate Change 2013: The Physical Science Basis,* T. F. Stocker et al., Eds., Cambridge University Press, 1029–1136.

de Vries, H., T. Woollings, J. Anstey, R. J. Haarsma, and W. Hazeleger, 2013: Atmospheric blocking and its relation to jet changes in a future climate. *Climate Dyn.,* **41,** 2643–2654, doi:10.1007/s00382-013-1699-7.

Dole, R., and N. Gordon, 1983: Persistent anomalies of the extratropical Northern Hemisphere wintertime circulation—Geographical distribution and regional persistence characteristics. *Mon. Wea. Rev.,* **111,** 1567–1586, doi:10.1175/1520-0493(1983)111<1567:PAOTEN>2.0.CO;2.

Dunn-Sigouin, E., and S.-W. Son, 2013: Northern Hemisphere blocking frequency and duration in the CMIP5 models. *J. Geophys. Res. Atmos.,* **118,** 1179–1188, doi:10.1002/jgrd.50143.

Erlebach, P., U. Langematz, and S. Pawson, 1996: Simulations of stratospheric sudden warmings in the Berlin troposphere-stratosphere-mesosphere GCM. *Ann. Geophys.,* **14,** 443–463, doi:10.1007/s00585-996-0443-6.

Garfinkel, C. I., D. L. Hartmann, and F. Sassi, 2010: Tropospheric precursors of anomalous Northern Hemisphere stratospheric polar vortices. *J. Climate,* **23,** 3282–3299, doi:10.1175/2010JCLI3010.1.

Hines, C. O., 1997a: Doppler-spread parameterization of gravity-wave momentum deposition in the middle atmosphere. Part 1: Basic formulation. *J. Atmos. Sol. Terr. Phys.,* **59,** 371–386, doi:10.1016/S1364-6826(96)00079-X.

——, 1997b: Doppler-spread parameterization of gravity-wave momentum deposition in the middle atmosphere. Part 2: Broad and quasi monochromatic spectra, and implementation. *J. Atmos. Sol.-Terr. Phys.,* **59,** 387–400, doi:10.1016/S1364-6826(96)00080-6.

Horel, J. D., and J. M. Wallace, 1981: Planetary-scale atmospheric phenomena associated with the Southern Oscillation. *Mon. Wea. Rev.,* **109,** 813–829, doi:10.1175/1520-0493(1981)109<0813:PSAPAW>2.0.CO;2.

Hu, Y., and K. K. Tung, 2003: Possible ozone-induced long-term changes in planetary wave activity in late winter. *J. Climate,* **16,** 3027–3038, doi:10.1175/1520-0442(2003)016<3027:POLCIP>2.0.CO;2.

Ineson, S., and A. A. Scaife, 2009: The role of the stratosphere in the European climate response to El Niño. *Nat. Geosci.,* **2,** 32–36, doi:10.1038/ngeo381.

Jöckel, P., and Coauthors, 2006: The atmospheric chemistry general circulation model ECHAM5/MESSy1: Consistent simulation of ozone from the surface to the mesosphere. *Atmos. Chem. Phys.,* **6,** 5067–5104, doi:10.5194/acp-6-5067-2006.

Julian, P. R., and K. B. Labitzke, 1965: A study of atmospheric energetics during the January–February 1963 stratospheric warming. *J. Atmos. Sci.,* **22,** 597–610, doi:10.1175/1520-0469(1965)022<0597:ASOAED>2.0.CO;2.

Jungclaus J., and Coauthors, 2013: Characteristics of the ocean simulations in the Max Planck Institute Ocean Model (MPIOM), the ocean component of the MPI-Earth System Model. *J. Adv. Model. Earth Syst.,* **5,** 422–446, doi:10.1002/jame.20023.

Kolstad, E. W., and A. J. Charlton-Perez, 2011: Observed and simulated precursors of stratospheric polar vortex anomalies in the Northern Hemisphere. *Climate Dyn.,* **37,** 1443–1456, doi:10.1007/s00382-010-0919-7.

Labitzke, K., 1981: Stratospheric–mesospheric midwinter disturbances: A summary of observed characteristics. *J. Geophys. Res.,* **86,** 9665–9678, doi:10.1029/JC086iC10p09665.

Lott, F., and M. J. Miller, 1997: A new subgrid-scale orographic drag parametrization: Its formulation and testing. *Quart. J. Roy. Meteor. Soc.,* **123,** 101–127, doi:10.1002/qj.49712353704.

Martius, O., L. M. Polvani, and H. C. Davies, 2009: Blocking precursors to stratospheric sudden warming events. *Geophys. Res. Lett.,* **36,** L14806, doi:10.1029/2009GL038776.

Masato, G., B. J. Hoskins, and T. Woolings, 2013: Winter and summer Northern Hemisphere blockings in CMIP5. *J. Climate,* **26,** 7044–7059, doi:10.1175/JCLI-D-12-00466.1.

McLandress, C., and T. G. Shepherd, 2009: Impact of climate change on stratospheric sudden warmings as simulated by the Canadian Middle Atmosphere Model. *J. Climate,* **22,** 5449–5463, doi:10.1175/2009JCLI3069.1.

Meinshausen, M., and Coauthors, 2011: The RCP greenhouse gas concentrations and their extensions from 1765 to 2300. *Climatic Change,* **109,** 213–241, doi:10.1007/s10584-011-0156-z.

Nakamura, H., M. Nakamura, and J. L. Anderson, 1997: The role of high- and low-frequency dynamics in blocking formation. *Mon. Wea. Rev.,* **125,** 2074–2093, doi:10.1175/1520-0493(1997)125<2074:TROHAL>2.0.CO;2.

Newman, P. A., and J. E. Rosenfield, 1997: Stratospheric thermal damping times. *Geophys. Res. Lett.,* **24,** 433–436, doi:10.1029/96GL03720.

——, E. R. Nash, and J. E. Rosenfield, 2001: What controls the temperature of the Arctic stratosphere during the spring? *J. Geophys. Res.,* **106,** 19 999–20 010, doi:10.1029/2000JD000061.

Nishii, K., H. Nakamura, and T. Miyasaka, 2009: Modulations in the planetary wave field induced by upward-propagating Rossby wave packets prior to stratospheric sudden warming events: A case-study. *Quart. J. Roy. Meteor. Soc.,* **135,** 39–52, doi:10.1002/qj.359.

——, ——, and Y. J. Orsolini, 2010: Cooling of the wintertime Arctic stratosphere induced by the western Pacific teleconnection pattern. *Geophys. Res. Lett.,* **37,** L13805, doi:10.1029/2010GL043551.

——, ——, and ——, 2011: Geographical dependence observed in blocking high influence on the stratospheric variability through enhancement and suppression of upward planetary-wave propagation. *J. Climate,* **24,** 6408–6423, doi:10.1175/JCLI-D-10-05021.1.

Nissen, K. M., K. Matthes, U. Langematz, and B. Mayer, 2007: Towards a better representation of the solar cycle in general circulation models. *Atmos. Chem. Phys.,* **7,** 5391–5400, doi:10.5194/acp-7-5391-2007.

Oberländer, S., U. Langematz, and S. Meul, 2013: Unraveling impact factors for future changes in the Brewer–Dobson circulation. *J. Geophys. Res. Atmos.,* **118,** 10 296–10 312, doi:10.1002/jgrd.50775.

Oman, L., D. W. Waugh, S. Pawson, R. S. Stolarski, and P. A. Newman, 2009: On the influence of anthropogenic forcings on changes in the stratospheric mean age. *J. Geophys. Res.,* **114,** D03105, doi:10.1029/2008JD010378.

Orsolini, Y. J., A. Karpechko, and G. Nikulin, 2009: Variability of the Northern Hemisphere polar stratospheric cloud potential: The role of North Pacific disturbances. *Quart. J. Roy. Meteor. Soc.,* **135,** 1020–1029, doi:10.1002/qj.409.

Polvani, L. M., and D. W. Waugh, 2004: Upward wave activity flux as a precursor to extreme stratospheric events and subsequent anomalous surface weather regime. *J. Climate,* **17,** 3548–3554, doi:10.1175/1520-0442(2004)017<3548:UWAFAA>2.0.CO;2.

Quiroz, R. S., 1986: The association of stratospheric warmings with tropospheric blocking. *J. Geophys. Res.,* **91,** 5277–5285, doi:10.1029/JD091iD04p05277.

Rex, D. F., 1950: Blocking action in the middle troposphere and its effect upon regional climate. *Tellus,* **2,** 196–211, doi:10.1111/j.2153-3490.1950.tb00331.x.

Roeckner, E., and Coauthors, 2006: Sensitivity of simulated climate to horizontal and vertical resolution in the ECHAM5 atmosphere model. *J. Climate,* **19,** 3771–3791, doi:10.1175/JCLI3824.1.

Sander, R., A. Kerkweg, P. Jöckel, and J. Lelieveld, 2005: Technical note: The new comprehensive atmospheric chemistry module MECCA. *Atmos. Chem. Phys.,* **5,** 445–450, doi:10.5194/acp-5-445-2005.

Scaife, A. A., T. Woollings, J. Knight, G. Martin, and T. Hinton, 2010: Atmospheric blocking and mean biases in climate models. *J. Climate,* **23,** 6143–6152, doi:10.1175/2010JCLI3728.1.

Sillmann, J., and M. Croci-Maspoli, 2009: Present and future atmospheric blocking and its impact on European mean and extreme climate. *Geophys. Res. Lett.,* **36,** L10702, doi:10.1029/2009GL038259.

Smith, K. L., and P. J. Kushner, 2012: Linear interference and the initiation of extratropical stratosphere–troposphere interactions. *J. Geophys. Res.,* **117,** D13107, doi:10.1029/2012JD017587.

Taguchi, M., 2008: Is there a statistical connection between stratospheric sudden warming and tropospheric blocking events? *J. Atmos. Sci.,* **65,** 1442–1454, doi:10.1175/2007JAS2363.1.

——, and D. L. Hartmann, 2006: Increased occurrence of stratospheric sudden warmings during El Niño as simulated by WACCM. *J. Climate,* **19,** 324–332, doi:10.1175/JCLI3655.1.

Takaya, K., and H. Nakamura, 2005: Geographical dependence of upper-level blocking formation associated with intraseasonal amplification of the Siberian high. *J. Atmos. Sci.,* **62,** 4441–4449, doi:10.1175/JAS3628.1.

Tibaldi, S., and F. Molteni, 1990: On the operational predictability of blocking. *Tellus,* **42,** 343–365, doi:10.1034/j.1600-0870.1990.t01-2-00003.x.

Vial, J., T. J. Osborn, and F. Lott, 2013: Sudden stratospheric warmings and tropospheric blockings in a multi-century simulation of the IPSL-CM5A coupled climate model. *Climate Dyn.,* **40,** 2401–2414, doi:10.1007/s00382-013-1675-2.

Wilks, D. S., 2011: *Statistical Methods in the Atmospheric Sciences*. 3rd ed. Academic Press, 676 pp.

WMO, 2007: Scientific assessment of ozone depletion: 2006. World Meteorological Organization Global Ozone Research and Monitoring Project Rep. 50. [Available online at http://ozone.unep.org/new_site/en/scientific_assessment_2006.php.]

Woollings, T., 2010: Dynamical influences on European climate: An uncertain future. *Philos. Trans. Roy. Soc. London,* **368A,** 3733–3756, doi:10.1098/rsta.2010.0040.

——, A. Charlton-Perez, S. Ineson, A. G. Marshall, and G. Masato, 2010: Associations between stratospheric variability and tropospheric blocking. *J. Geophys. Res.,* **115,** D06108, doi:10.1029/2009JD012742.